frontiers | Frontiers in Energy Research

ORIGINAL RESEARCH
published: 25 August 2022
doi: 10.3389/fenrg.2022.893528

A Model Predictive Controller for the Core Power Control System of a Lead-Cooled Fast Reactor

Yang Hu, Lehua Liang, Lekang Chen and Wenjie Zeng*

School of Nuclear Science and Technology, University of South China, Hengyang City, China

To study the model predictive control (MPC) for a lead-cooled fast reactor's core power control system (LFR), firstly, the LFR core is established with the state space model. Then, to establish an LFR core power control system, a predictive model controller is used. Finally, the conditions of 20pcm step reactivity and 5% step down of coolant inlet temperature are introduced to study the control characteristic. The maximum overshot (MO) and the transient time are calculated in the time domain, and the stability of the core power control system is analyzed using the Nyquist and Bode diagrams in frequency domains. The result shows that the MPC controller and PID controller are feasible in core power control, and the core power control systems are closed-loop stable systems.

Keywords: model predictive control, core power control system, lead-cooled fast reactor, stability, state space model

OPEN ACCESS

Edited by:
Xinyu Wei,
Xi'an Jiaotong University, China

Reviewed by:
Qian Zhang,
Harbin Engineering University, China
Rui Wang,
Northeastern University, China
Zhou Shiliang,
North China Electric Power University, China

***Correspondence:**
Wenjie Zeng
zengwenjie0218@163.com

Specialty section:
This article was submitted to Nuclear Energy, a section of the journal Frontiers in Energy Research.

Received: *10 March 2022*
Accepted: *30 May 2022*
Published: *25 August 2022*

Citation:
Hu Y, Liang L, Chen L and Zeng W (2022) A Model Predictive Controller for the Core Power Control System of a Lead-Cooled Fast Reactor. Front. Energy Res. 10:893528. doi: 10.3389/fenrg.2022.893528

1 INTRODUCTION

Lead-cooled fast reactors (LFRs), one of the candidate reactor types in the fourth generation of nuclear power systems that show the most potential, are under investigation for their high security and easy miniaturization. LFRs use liquid lead or lead alloy with a high boiling point and high thermal conductivity as a coolant, which not only has a hard neutron energy spectrum but also effectively improves the reactor's safety limit and operation range (Xiuzhong, 2002). Therefore, LFR has a good neutron economy and safety (Lorenzi et al., 2013).

The fast reactor has a small delayed neutron share, short prompt neutron lifetime, and weak Doppler effect. Under reactivity disturbance, the reactor power changes rapidly because of poor self-balancing ability. Therefore, the fast reactor controller requires a more rapid response speed and higher control accuracy. Linear Active Disturbance Rejection Control with and without model information has been established to meet this demand. Both have fast regulation speed and accuracy for the power control system of LFR (Shen, 2019). To resist external interference and parameter uncertainty, a synovial control method based on robust nonlinear control was established (Ansarifar et al., 2016). While some tracking controllers use only the current tracking command, the predictive model controllers can achieve better tracking performance because future commands are considered in addition to the current tracking command (Na et al., 2005). Based on the advantages of MPC, a predictive model controller for the load-following operation of a pressurized water reactor was designed. The controller was approved using the three-dimensional nuclear reactor analysis code master developed by Korea Atomic Energy Research Institute (Na et al., 2005). A nonlinear model predictive controller for variable load process of High-Temperature Gas-cooled was established, which overcomes the problems of system coupling, nonlinearity, and time-varying parameters of new nuclear power plant HTR-PM

(Song, 2012). The core power control of a fast reactor cannot be satisfied by a traditional PID controller. Traditional PID controllers cannot fulfill the core power control of a fast reactor. In this work, the advanced control strategy predictive model control was used to design the controller to study the core power control of a fast reactor. The advantage of the MPC controller lies in its good tracking performance and rolling optimization characteristics.

The remaining parts of thisarticle are organized in the following sequence. In **section 2**, the linear system model of LFR is established by the lumped parameter method, and the simulation system based on the state space model is designed. Section 3 introduces the core power control system with an MPC controller for LFR. Section 4 shows a simulated response of the core power control system under reactivity insertion accident and coolant inlet temperature disturbance, and the Nyquist and Bode diagram are drawn. Finally, **section 5** has our conclusions.

2 DYNAMIC MODEL OF LFR CORE

2.1 The Nonlinear Model of Reactor Core

Based on the point reactor neutron dynamics with six groups of effective delayed neutron and thermal-hydraulic coupling methods, taking into account the reactivity feedback caused by the temperature change of core coolant, fuel, and cladding, the ordinary differential equations are shown in **Eq. 1** to describe the nonlinear model of LFR core (Lorenzi et al., 2013).

$$\begin{cases} \frac{\mathrm{d}C_i(t)}{\mathrm{d}t} = \frac{\beta_i}{\Lambda}\cdot N_r(t) - \lambda_i\cdot C_i(t), i = 1,2\ldots 6 \\ \frac{\mathrm{d}N_r(t)}{\mathrm{d}t} = \frac{\rho(t)-\beta}{\Lambda}\cdot N_r(t) + \sum_{i=1}^{6}\lambda_i\cdot C_i(t) \\ M_f\cdot C_f\frac{dT_f}{dt} = P(t) - U_{f,c}\left(T_f - T_c\right) \\ M_c\cdot C_c\cdot\frac{dT_c}{dt} = U_{f,c}\left(T_f - T_c\right) - U_{c,ave}(T_c - T_{ave}) \\ M_{ave}\cdot C_{ave}\cdot\frac{dT_{ave}}{dt} = U_{c,ave}(T_c - T_{ave}) - 2G(t)\cdot C_{ave}\cdot(T_{ave} - T_{in}) \\ \rho(t) = \rho_{rod} + \alpha_f\left(T_f - T_{ave}\right) + \alpha_c(T_c - T_{c0}) + \alpha_{ave}(T_{ave} - T_{ave0}) + \alpha_{in}(T_{in} - T_{in0}) \\ \rho_{rod} = \alpha_{rod}\triangle h \end{cases} \tag{1}$$

where the relationship between relative core power and relative neutron density should conform to **Eq. 2**.

$$\begin{cases} N_r(t) = \frac{N(t)}{N_0}, P_r(t) = \frac{P(t)}{P_0} \\ N_r(t) = P_r(t) \end{cases} \tag{2}$$

2.2 The State Space Model of Reactor Core

The linear model is established based on the nonlinear reactor core model by introducing small perturbations and ignoring the high-order term (Li and Zhao, 2013; Yinuo, 2021). The ordinary differential equations are shown in **Eq. 3**

$$\begin{cases} \frac{d\delta P_r(t)}{dt} = \frac{\rho_0-\beta}{\Lambda}\delta P_r(t) + \sum_{i=1}^{6}\lambda\delta C_i + \frac{\rho_{rod} + \alpha_f\delta T_f + \alpha_c\delta T_c + \alpha_{ave}\delta T_{ave} + \alpha_{in}\delta T_{in}}{\Lambda}P_{r0} \\ \frac{d\delta C_i(t)}{dt} = \frac{\beta_i}{\Lambda}\delta P_r - \lambda\delta C_i(t), i = 1,2\ldots 6 \\ M_f C_{p,f}\frac{d\delta T_f}{dt} = \delta P_r(t)P_0 - U_{f,c}\left[\delta T_f(t) - \delta T_c(t)\right] \\ M_c C_{p,c}\frac{d\delta T_c}{dt} = U_{f,c}\left(\delta T_f - \delta T_c\right) - U_{c,ave}(\delta T_c - \delta T_{ave}) \\ M_{ave}C_{p,ave}\frac{d\delta T_{ave}}{dt} = U_{c,ave}(\delta T_c - \delta T_{ave}) - 2GC_{p,ave}(\delta T_{ave} - \delta T_{in}) \end{cases} \tag{3}$$

Following **Eq. 3**, the state space model of the reactor core is obtained as **Eq. 4**.

$$\begin{cases} \dot{x} = \boldsymbol{A}x + \boldsymbol{B}u \\ y = \boldsymbol{C}x + \boldsymbol{D}u \end{cases} \tag{4}$$

where $\boldsymbol{u} = [\delta\rho_{rod}, T_{in}]^T$ is the input, $\mathbf{y} = [\delta P_r, \delta T_f, \delta T_c, \delta T_{ave}]^T$ is the output, $\boldsymbol{x} = [x_1, x_2, x_3, x_4, x_5, x_6, x_7, x_8, x_9, x_{10}]^T = [\delta P_r, \delta C_1, \delta C_2, \delta C_3, \delta C_4, \delta C_5, \delta C_6, \delta T_f, \delta T_c, \delta T_{ave}]^T$ is the $R^{10\times 10}$ state array, $\boldsymbol{A}$ is the $R^{10\times 10}$ system matrix, $\boldsymbol{B}$ is the $R^{10\times 2}$ input matrix; $\boldsymbol{C}$ is the $R^{4\times 10}$ output matrix, $\boldsymbol{D}$ is the $R^{10\times 2}$ zero matrix. $\boldsymbol{A}$, $\boldsymbol{B}$, $\boldsymbol{C}$, and $\boldsymbol{D}$ are represented by

$$\boldsymbol{A} = \begin{bmatrix} \frac{\rho_0-\beta}{\Lambda} & \lambda_1 & \lambda_2 & \lambda_3 & \lambda_4 & \lambda_5 & \lambda_6 & \frac{P_{r0}}{\Lambda}\cdot\alpha_f & \frac{P_{r0}}{\Lambda}\cdot\alpha_c & \frac{P_{r0}}{\Lambda}\cdot\alpha_{ave} \\ \frac{\beta_1}{\Lambda} & -\lambda_1 & 0 & 0 & 0 & 0 & 0 & 0 & 0 & 0 \\ \frac{\beta_2}{\Lambda} & 0 & -\lambda_2 & 0 & 0 & 0 & 0 & 0 & 0 & 0 \\ \frac{\beta_3}{\Lambda} & 0 & 0 & -\lambda_3 & 0 & 0 & 0 & 0 & 0 & 0 \\ \frac{\beta_4}{\Lambda} & 0 & 0 & 0 & -\lambda_4 & 0 & 0 & 0 & 0 & 0 \\ \frac{\beta_5}{\Lambda} & 0 & 0 & 0 & 0 & -\lambda_5 & 0 & 0 & 0 & 0 \\ \frac{\beta_6}{\Lambda} & 0 & 0 & 0 & 0 & 0 & -\lambda_6 & 0 & 0 & 0 \\ \frac{P_0}{M_f C_{p,f}} & 0 & 0 & 0 & 0 & 0 & 0 & -\frac{U_{f,c}}{M_f C_{p,f}} & \frac{U_{f,c}}{M_f C_{p,f}} & 0 \\ 0 & 0 & 0 & 0 & 0 & 0 & 0 & \frac{U_{f,c}}{M_c C_{p,c}} & -\frac{U_{f,c}+U_{c,ave}}{M_c C_{p,c}} & \frac{U_{c,ave}}{M_c C_{p,c}} \\ 0 & 0 & 0 & 0 & 0 & 0 & 0 & 0 & \frac{U_{c,ave}}{M_{ave}C_{p,ave}} & -\frac{U_{c,ave}+2GC}{M_{ave}C_{p,ave}} \end{bmatrix}$$

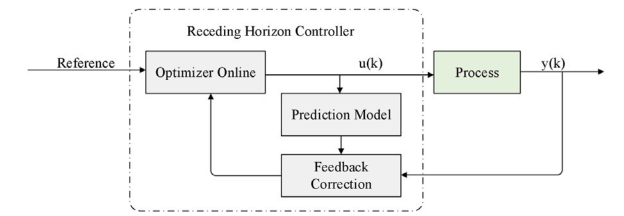

FIGURE 1 | Schematic block diagram of the MPC controller.

$$B = \begin{bmatrix} \frac{P_{r0}}{\Lambda} & 0 \\ 0 & 0 \\ 0 & 0 \\ 0 & 0 \\ 0 & 0 \\ 0 & 0 \\ 0 & 0 \\ 0 & 0 \\ 0 & 0 \\ 0 & 2GC \end{bmatrix}$$

$$C = \begin{bmatrix} 1 & 0 & 0 & 0 & 0 & 0 & 0 & 0 & 0 & 0 \\ 0 & 0 & 0 & 0 & 0 & 0 & 0 & 1 & 0 & 0 \\ 0 & 0 & 0 & 0 & 0 & 0 & 0 & 0 & 1 & 0 \\ 0 & 0 & 0 & 0 & 0 & 0 & 0 & 0 & 0 & 1 \end{bmatrix} D = \begin{bmatrix} 0 & 0 & 0 & 0 \\ 0 & 0 & 0 & 0 \\ 0 & 0 & 0 & 0 \\ 0 & 0 & 0 & 0 \end{bmatrix}$$

3 DESIGN OF A REACTOR CORE POWER CONTROL SYSTEM WITH MPC CONTROLLER

3.1 The Basic Principle of MPC Controller

Model predictive control (MPC), also known as receding horizon control, has gained attention in academia and industry due to its ability to optimally control nonlinear systems subject to physical constraints (Brian Froisy, 1994; Mayne, 2000; Hu and Ding, 2019). The structure of the MPC controller is shown in **Figure 1**.

3.1.1 Predictive Model

The output of predictive model control depends not only on the input and output of the control system but also on the control variables of the controller output. The essence of model prediction is to establish the relationship between historical output and the future output of the control system (Na et al., 2005; Chen, 2013).

(1) Ignoring the input measurable interference to simplify the model, the discrete-time state-space model incremental formula is introduced:

$$\begin{cases} \Delta x(k+1) = A \cdot \Delta x(k) + B \cdot \Delta u(k) \\ y(k) = C \cdot \Delta x(k) + y(k-1) \end{cases} \tag{5}$$

where A, B, C, and D are paraments of the MPC controller, x is the internal variable, u is the control variable, and y is the control system's output

(2) Based on the discrete-time state space model, we set p as the prediction time and m as the control time, then at the time p:

$$\begin{cases} \Delta x(k+p|k) = A^p \cdot \Delta x(k) + \sum_{i=1}^{p} A^{m-i} \cdot B \cdot \Delta u(k+p-i) \\ y(k+p|k) = \sum_{i=1}^{p} A^i \cdot \Delta x(k) + \sum_{j=0}^{p-1} \sum_{i=1}^{p-j} C \cdot A^{i-1} \cdot \Delta u(k+j) \end{cases} \tag{6}$$

(3) Predicted output of the reactor core power control system in the next p

step, $\boldsymbol{Y}_{\mathrm{p}}(k+m|k) = \boldsymbol{S}_{\mathrm{x}} \cdot \Delta x(k) + \boldsymbol{I} \cdot y(k) + \boldsymbol{S}_{\mathrm{u}} \cdot \Delta u(k)$ (7)

where $(k+p|k)$ indicates the status of the forecast of the time $(p + k)$ at the time p,

$$\begin{cases} \boldsymbol{Y}_{\mathrm{p}}(k+1|k) = \begin{pmatrix} y(k+1|k) \\ \vdots \\ y(k+p|k) \end{pmatrix} \\ \boldsymbol{\Delta u} = \begin{pmatrix} \Delta u(k) \\ \vdots \\ \Delta u(k+m-1) \end{pmatrix} \\ \boldsymbol{S}_{\mathrm{x}} = \begin{pmatrix} CA \\ \sum_{i=1}^{2} CA^i \\ \vdots \\ \sum_{i=1}^{p} CA^i \end{pmatrix} \quad \boldsymbol{I} = \begin{pmatrix} I_n \cdot n \\ \vdots \\ I_n \cdot n \end{pmatrix} \\ \boldsymbol{S}_{\mathrm{u}} = \begin{pmatrix} CB & 0 & 0 & \cdots & 0 \\ \sum_{i=1}^{p} CA^{i-1}B & CB & \vdots & \vdots & 0 \\ \vdots & \cdots & \cdots & \ddots & 0 \\ \sum_{i=1}^{p} CA^{i-1}B & \sum_{i=1}^{p-1} CA^{i-1}B & \cdots & \cdots & BC \end{pmatrix}_{p\times m} \end{cases} \tag{8}$$

3.1.2 Rolling Optimization

Based on the model prediction, the most important feature of MPC is rolling optimization, which repeatedly solves the performance index J online$\frac{dJ(\Delta u)}{d\Delta u} = 0$. To achieve the receding horizon control of the system, the optimization problem is refreshed with the latest measured value at each sampling time by multiplying it with the shift matrix $\boldsymbol{L}$.

$$\begin{cases} J = \left(Y - Y_{ref}\right)^T \cdot Q \cdot \left(Y - Y_{ref}\right) + \Delta u^T \cdot R \cdot \Delta u \\ \boldsymbol{L} = \begin{pmatrix} 010\cdots0 \\ 001\cdots0 \\ \vdots\cdots\vdots\ddots 1 \\ 000\cdots1 \end{pmatrix} \end{cases} \tag{9}$$

3.1.3 Feedback Correction

Based on model prediction and receding horizon control, to prevent decreasing adaptability of the MPC to the controlled object under external interference, the model predictive output is further modified to be the input of receding horizon control, forming a closed-loop control system.

3.2 Operation Strategy of Stable Core Power With MPC Controller

As shown in **Figure 2**, the I/V converter converts reactor core power into voltage signal *V(n)* to be the feedback signal of the core power control system with the MPC controller, and the MPC

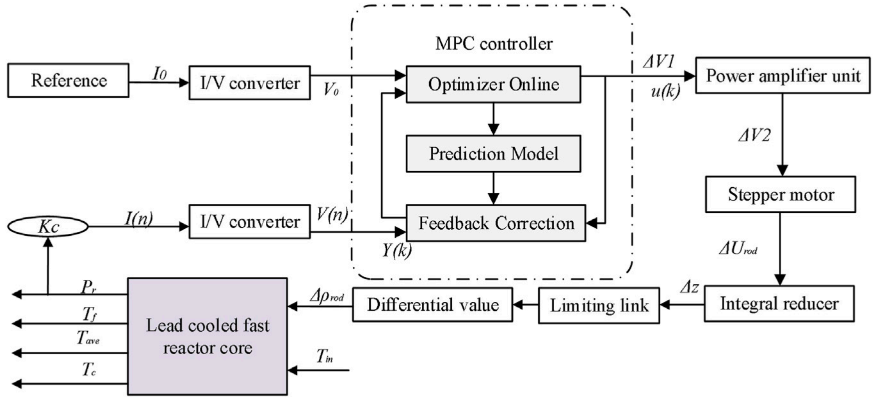

FIGURE 2 | LFR core power control system with MPC controller.

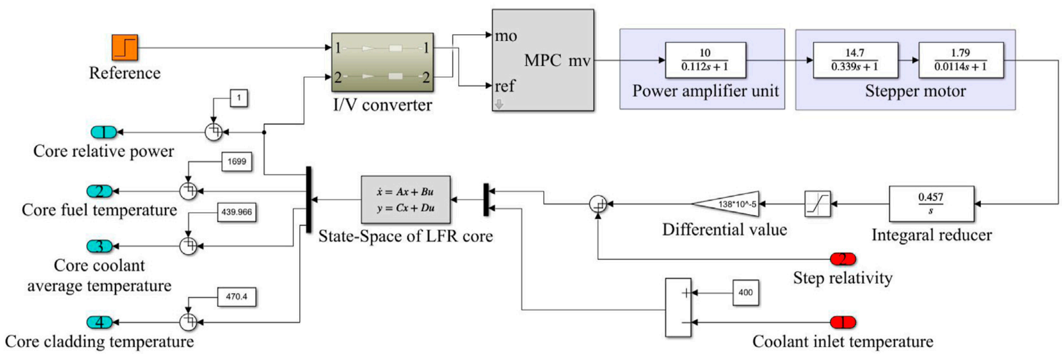

FIGURE 3 | Core power control system with MPC controller of LFR.

controller regulates the electrical signal and outputs to the control rod drive mechanism. The control rod drive mechanism drives the control rod to move in the reactor according to the relative power deviation. Inserting or withdrawing reactivity in the reactor adjusts the reactor power back to the setting value and finally makes the core power stable (Hu, 2021; Yinuo, 2021). As shown in **Figure 3**, based on the operation strategy of stable core power with MPC controller, the core power control simulation system with MPC controller is designed by using the MPC design module of MATLAB/Simulink, taking 0.1s as the sample time. The $V(n)$ of the core power system is the $\boldsymbol{Y}$ and the $\Delta V1$ is $\Delta\mathbf{u}$ of the MPC controller.

4 SIMULATION AND ANALYSIS

To compare the control characteristic of the MPC controller and PID controller, firstly, we set the parameters of the PID controller by a trial-and-error method. The parameters K_p, K_i, and K_d of the controller are 0.067, 0.0123, and 0.0006 through the continuous test. Then 20pcm step reactivity and the 5% step down of coolant inlet temperature are carried out. To compare the dynamic characteristics of a reactor core power control system with MPC and PID controller, the maximum overshot (MO) and the transient time are calculated in the time domain. The Nyquist and Bode diagram are drawn in a frequency domain to analyze their stability.

4.1 Time Domain Analysis of a LFR Core Power Control System

At 100%FP, the response of the LFR core under the power control system with 20 pcm step reactivity is shown in **Figure 4**. **Figure 5** shows the response of the LFR core power control system under the 5% step down of coolant inlet temperature. With the MPC controller or the PID controller, relative core power, core fuel temperature, core coolant average temperature, and core-cladding temperature finally return to the initial level, introducing step reactivity. In **Figures 4**, **5**, although both have great control characteristics, the dynamic characteristics of the core power control system with MPC controller are better than the PID controller in terms of MO and transient time.

4.2 Frequency Domain Analysis of an LFR Core Power Control System

In the frequency domain, the core power control system is linearized using the APP linearize model in MATLAB/Simulink, and the Nyquist diagram, Pole-Zero Map , and

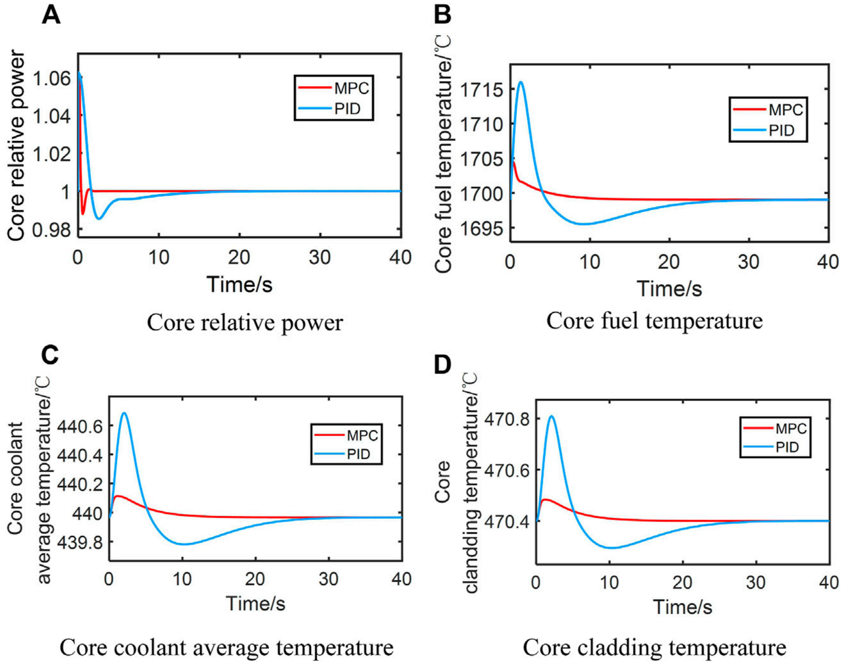

FIGURE 4 | Response of an LFR core power control system after introducing 20 pcm step reactivity.

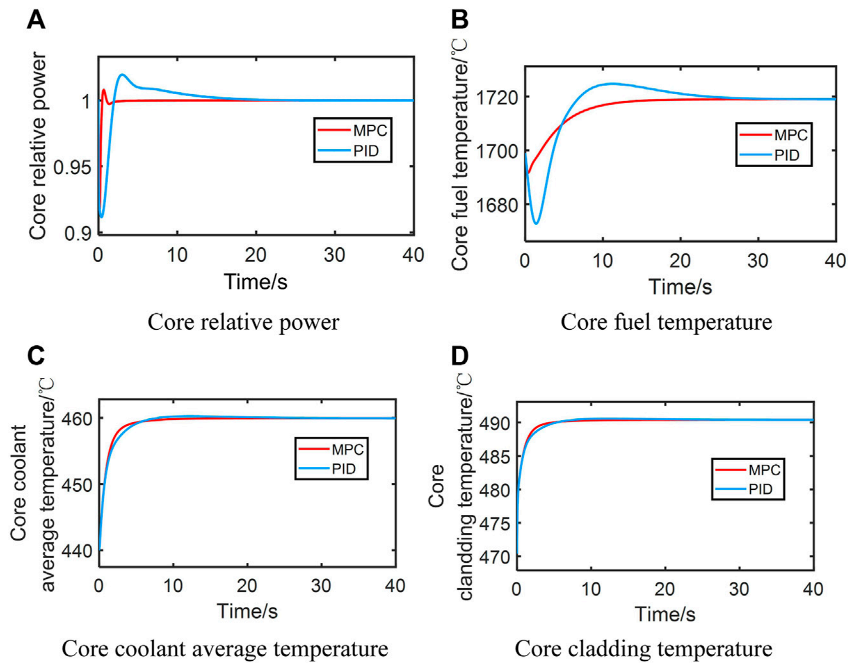

FIGURE 5 | Response of an LFR core power control system after introducing a 5% step down of core coolant inlet temperature.

Bode diagram are drawn. As shown in **Figures 6**, **7**, the Nyquist diagram and Pole-Zero Map are drawn to judge the absolute stability of the core power control system. According to the Nyquist diagram, the number of times that the Nyquist curve bypasses point (−1,0) counterclockwise is zero, and the number of characteristic roots outside the unit circle is zero. According to the Nyquist criterion, both closed-loop systems are stable. And as shown in **Figure 8**, the Bode diagram is drawn to compare the relative stability of different core power control systems. It can be seen from the Bode diagram that

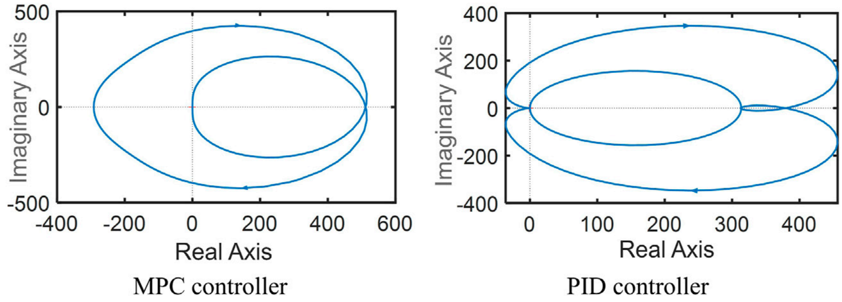

FIGURE 6 | Nyquist diagram of the core power control system.

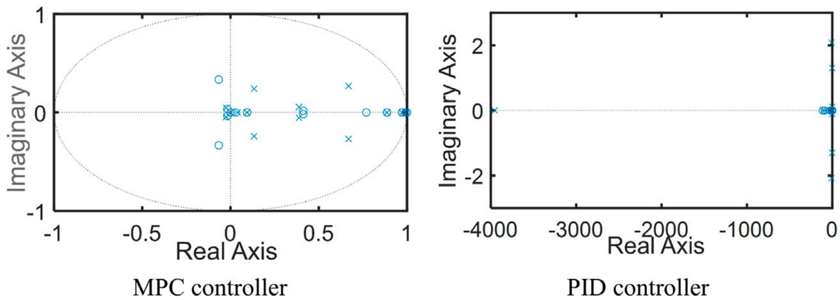

FIGURE 7 | Pole-Zero map of the core power control system. Note: MPC controller is indicated in the blue line, and PID controller is shown in the red line.

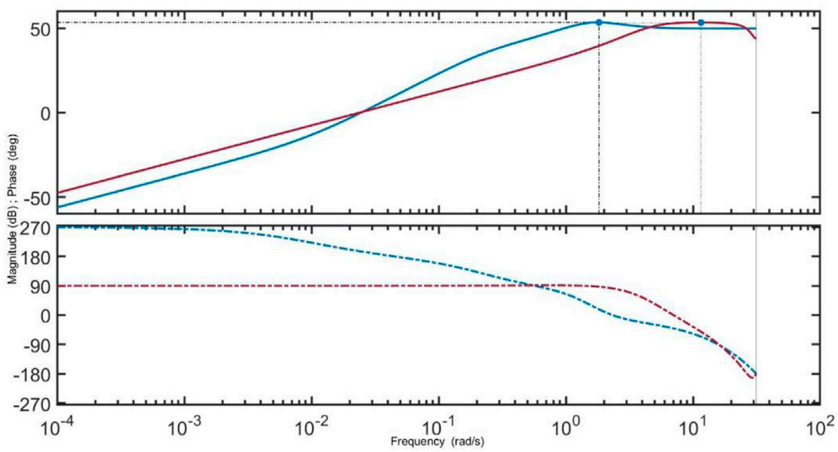

Note: MPC controller is indicated by blue line, and PID controller is indicated by red line

FIGURE 8 | Bode diagram of a core power control system with MPC and PID controller.

both phase margin and gain margin are stable in the low-frequency region.

5 CONCLUSION

The core power control system of the lead-cooled fast reactor is designed with the predictive model controller. According to the point reactor dynamics, the state space model of LFR is established using the perturbation theory. The core power control systems with MPC controller and PID controller are designed under the operation strategy of stable core power. We found that the control characteristic of the core power control system with MPC controller is better than the core power control system with PID controller. Both core power control systems with MPC controller and PID controller are stable. The concept of a core power system with an MPC controller and its control characteristic and stability of it is given in this research and can provide theoretical references for engineering applications.

DATA AVAILABILITY STATEMENT

The original contributions presented in the study are included in the article/Supplementary Materials, and further inquiries can be directed to the corresponding author.

AUTHOR CONTRIBUTIONS

YH: experimental data analysis, writing—original draft. LL: visualization, investigation. LC: project review. WZ: supervision, writing—review and editing.

FUNDING

The work was partly supported by the Provincial Innovation and Entrepreneurship Training Program for Undergraduates (S202210555135, S202210555133).

REFERENCES

Ansarifar, G. R., Nasrabadi, M., and Hassanvand, R. (2016). Core Power Control of the Fast Nuclear Reactors with Estimation of the Delayed Neutron Precursor Density Using Sliding Mode Method. *Nucl. Eng. Des.* 296, 1–8. doi:10.1016/j.nucengdes.2015.10.015

Brian Froisy, J. (1994). Model Predictive Control: Past, Present and Future. *ISA T* 33, 235–243. doi:10.1016/0019-0578(94)90095-7

Chen, H. (2013). *Model Predictive Control*. Beijing: Science Press, 14–17.

Hu, J., and Ding, B. (2019). Output Feedback Robust MPC for Linear Systems with Norm-Bounded Model Uncertainty and Disturbance. *Automatica* 108, 108489. doi:10.1016/j.automatica.2019.07.002

Hu, Y. (2021). Modelling and Simulation of the Primary System for a Small Lead-Cooled Fast Reactor with a Ratio of Core Power to Flow. *Ann. Nucl. Energy* 2022, 167. doi:10.1016/j.anucene.2021.11.01

Li, G., and Zhao, F. (2013). Flexibility Control and Simulation with Multi-Model and LQG/LTR Design for PWR Core Load Following Operation. *Ann. Nucl. Energy* 56, 179–188. doi:10.1016/j.anucene.2013.01.035

Lorenzi, S., Ponciroli, R., Cammi, A., and Bortot, S. (2013). Development of a Control-Oriented Simulator for a LFR Demonstrator. *Nucl. Eng. Des.* 262, 319–339. doi:10.1016/j.nucengdes.2013.04.027

Mayne, D. Q. (2000). Constrained Model Predictive Control: Stability and Optimality. *Automatica* 36, 789–814. doi:10.1016/s0005-1098(00)00173-4

Na, M. G., Jung, D. W., Shin, S. H., Jang, J. W., Lee, K. B., and Lee, Y. J. (2005). A Model Predictive Controller for Load-Following Operation of PWR Reactors. *IEEE Trans. Nucl. Sci.* 52 (5), 1009–1020. doi:10.1109/TNS.2005.852651

Shen, C. (2019). Linear Active Disturbance Rejection Control for Lead-Cooled Fast Reactor Power. *Nucl. Sci. Eng.* 39 (3), 337–344. doi:10.3969/j.issn.0258-0918.2019.03.001

Song, H. (2012). A Model Predictive Controller for Load-Following Operation of High Temperature Gas Cooled Reactor. *Comput. Appl. Chem.* 29 (1), 49–55. doi:10.1109/TNS.2005.852651

Xiuzhong, S. (2002). Analysis of Inherent Safety of Lead Cooled Fast Reactor. *Nucl. Power Eng.* (04), 75–78. doi:10.1016/j.jnucmat.2011.04.038

Yinuo, L. (2021). Uncertainty Analysis of Reactivity Feedback Coefficient for LFR Core Power Control System during Reactivity Insertion Accident. *Ann. Nucl. Energy.* 160, 108401. doi:10.1016/j.anucene.2021.108401

Conflict of Interest: The authors declare that the research was conducted without any commercial or financial relationships that could be interpreted as a potential conflict of interest.

GLOSSARY

t time

T temperature

h control rod position

C precursor density

N neutron density

P core power

M mass

C_p specific heat capacity at constant pressure

G coolant mass flow

U heat transfer coefficient

p prediction horizon

m control horizon

k discrete variable

Greek Symbols

ρ reactivity

β total delayed neutron fraction

λ decay constant

Λ neutron generation time

α reactivity feedback coefficient

δ small perturbation

Δ variation

Subscripts

r value relative to the initial value

f fuel

c cladding

ave average

in inlet

rod control rod

0 initial value

Abbreviations

LFR lead-cooled fast reactor

MPC model predictive control

MO maximum overshot

FP full power

PID proportional-integral-derivative